

detected at the age of 3 days. Physical examination revealed no hepatosplenomegaly. The patient suffered from bloody stool from the age of 9 to 56 days. Peripheral blood analysis at the age of day 42 disclosed an increased white blood cell count (WBC) of $35.5 \times 10^9/L$ with myeloblasts (3%), myeloid/erythroid precursors and monocytosis ($9.2 \times 10^9/L$), hemoglobin of 8.9 g/dL, and a platelet count of $44 \times 10^9/L$. The mean platelet volume was not evaluated but the morphology of the platelets showed anisocytosis with occasional giant platelets. Laboratory studies disclosed an elevated lactate dehydrogenase (826 IU/L, normal range: 233 to 391 IU/L), negative cytomegalovirus (CMV) IgM, and positive CMV IgG titer (possibly maternal antibody transfer) by enzyme-linked immunoassay.

The bone marrow was normocellular for age with a significant predominance of myelopoiesis (M/E ratio = 60) with a left shift of the myeloid lineage. The number of megakaryocytes was normal, but they were slightly dysplastic with hypolobulated nuclei. Dysplasia was not prominent in myeloid and erythroid lineages. The karyotype was normal (46, XY). From these features, the diagnosis of JMML was considered. The in vitro culture study demonstrated spontaneous granulocyte/macrophage colony formation. However, the assay of GM-CSF hypersensitivity could not be done because of insufficient materials. Molecular analysis of PTPN11, N-ras, and K-ras genes, which was performed as previously reported, documented no mutation and there was no family history of neurofibromatosis type 1.¹¹ The diagnosis of JMML was made according to the international criteria.⁷ Subsequently, the WBC count increased up to $52.0 \times 10^9/L$ with persistent fever, which was unresponsive to antibiotics. Oral 6-mercaptopurine (2 mg/kg) was started at the age of 44 days, which resolved the hyperleukocytosis and fever. At the age of 7 months, he was referred to the Japanese Red Cross Nagoya First Hospital for hematopoietic stem cell transplantation. Physical examination revealed atopic dermatitis-like eczema on the face and trunk, mild hepatomegaly (3 cm under the right costal margin), but no splenomegaly. Under 6-mercaptopurine therapy, peripheral blood analysis disclosed a WBC count of $12.9 \times 10^9/L$ with monocytosis ($1.9 \times 10^9/L$). Laboratory studies revealed elevated IgG (2554 mg/dL) and IgE (494 IU/mL), low IgA (49 mg/dL) and normal IgM (156 mg/dL). The value of HbF was within the normal range for age (6.0%). Positive results of CMV-IgM/IgG and pp65 CMV-Ag (5 positive cells among 100,000 cells) were noted without CMV-related symptoms and intravenous administration of ganciclovir was

initiated. Evaluation of T-cell function revealed normal responses to phytohemagglutinin and concanavalin A. The number of peripheral T and B cells and CD4/8 ratio were also normal.

Although the patients fulfilled the diagnostic criteria of JMML, the presence of atopic dermatitis-like eczema led to the consideration of WAS. FCM-WASP was performed as previously described and the result revealed the lack of WASP expression.¹² Sequencing of WASP cDNA identified 5 nucleotides (CCGGG) inserted at position 462 in exon 4, causing a frameshift at codon 140 that gives rise to a premature stop signal at codon 262. The sequences of genomic DNA of the WASP gene from the patient's mother and his brother who was born 1 year later did not show any mutations (data not shown), indicating that it arose de novo. It was also lacking in $100 \times$ chromosomes from healthy unrelated adults screened for this mutation. The diagnosis of WAS was confirmed.

He underwent cord blood transplantation at the age of 10 months. The patient has survived for more than 6 months in good clinical condition. FCM-WASP at day 90 showed the normal expression of WASP (Fig. 1).

DISCUSSION

Here we reported a male infant with WAS who experienced an unusual clinical course, which fulfilled the diagnostic criteria of JMML. This is the first report on a JMML-like disorder in a patient with WAS, as far as we know. Detection of giant platelets instead of microthrombocytes, which is the only specific clinical sign of WAS, and failure to demonstrate immune defects by immunologic screening tests such as serum IgG, IgM, and IgA concentrations, lymphocyte subsets, and in vitro lymphocyte proliferation to mitogens (phytohemagglutinin or concanavalin A), made the diagnostic approach difficult. Without recent advances in the diagnostic tests of WAS, including FCM-WASP and WASP gene analysis, it might have been impossible to reach the diagnosis of WAS in this patient. Presentation since birth and some clinical features including atopic dermatitis-like eczema, bloody stool (presumably as a result of WAS-associated colitis), lack of splenomegaly, and normal value of HbF were unusual for JMML but compatible with WAS.

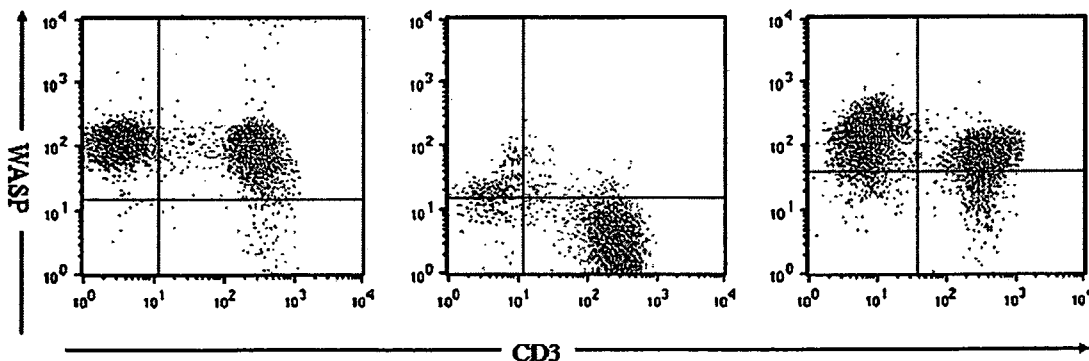


FIGURE 1. Analysis of 2-color FCM-WASP. Density plots are from 2-color FCM-WASP using CD3 antibody. All cells in the lymphocyte gate were analyzed. The x-axis represents CD3 intensity; y-axis represents WASP intensity. WASP expression is shown in lymphocytes from a healthy control (right), a WAS patient before hematopoietic stem cell transplantation (middle), and a patient after hematopoietic stem cell transplantation (data on day 90 after cord blood stem cell transplantation).

Patients with WAS are known to have a predisposition to malignancy, commonly lymphoma.¹ There have been no reports on myeloid malignancy. Recently, however, 2 reports were published which described "myelodysplasia" in patients with WASP-related diseases. The first was reported by Imai et al,¹³ which summarized the clinical course of 50 patients with classic WAS and included 3 patients who presented with myelodysplasia. Interestingly, the patients were also very young (0.1, 0.2, and 3 years old). These 3 patients had splenomegaly with or without hepatomegaly (Dr Kosuke Imai, personal communication, March 2007), which suggests the myeloproliferative nature of the disease and myelodysplasia. Ancliff et al⁴ reported a 4-year-old patient with a novel type of WASP mutation who presented with severe neutropenia and trilineage dysplasia with excess blasts in the bone marrow. The patient had activating mutation of WASP which increased WASP activity.⁴ The pathogenesis of myelodysplasia in these patients are unknown.

In JMML, the GM-CSF/RAS pathway has the central role in pathogenesis and *PTPN11*, *RAS*, and *NF-1* are involved in this pathway; however, there is no known functional relationship between WASP and the GM-CSF/RAS pathway. WASP plays an important role in the transduction of signals from the cell surface to the actin cytoskeleton. Although WASP is expressed ubiquitously in hematopoietic cells and in vitro results suggest that WASP is involved in the proliferation and differentiation of hematopoietic progenitors, overt functional defects are restricted to thrombocytes and leukocytes in classic WAS, and the role of WASP in erythropoiesis and myelopoiesis is poorly defined.^{14,15} Further investigation of the functions of WASP in hematopoiesis may be helpful to elucidate the underlying mechanism of JMML-like features and myelodysplasia in WAS patients.

As CMV antigenemia was detected in this patient, it is possible to assume that CMV caused the JMML-like features. It is reported that viral infections including CMV mimic JMML.¹⁶⁻¹⁹ As concomitant viral infections are often noted in JMML patients, it is not straightforward to distinguish them from JMML. In the patient reported here, CMV antigenemia was detected only once without any additional clinical symptoms and there was no significant change in the clinical features before and after the detection of CMV antigenemia or administration of ganciclovir; therefore, we believe that CMV did not play a central role in the pathogenesis in this patient.

Recent advances in our understanding of the molecular pathogenesis of JMML have dramatically changed our diagnostic approach, and mutational analyses of *PTPN11* and *RAS* genes have become routine diagnostic tests; however, in 20% to 30% of patients without any molecular markers, the diagnosis of JMML still relies on nonspecific clinical and laboratory observations. Therefore, careful differential diagnosis of diseases presenting with similar clinical and morphologic features is needed, such as viral infections and leukocyte adhesion deficiency type 1.¹⁶⁻²⁰ We suggest that WAS should be

considered an important differential diagnosis in male infants with clinical features of JMML, even if microthrombocytes could not be demonstrated.

ACKNOWLEDGMENTS

The authors are grateful to Ms Yoshie Miura for excellent technical assistance, and Drs Tomohiro Morio and Kohsuke Imai for helpful discussions.

REFERENCES

- Sullivan KE, Mullen CA, Blaise RM, et al. A multiinstitutional survey of the Wiskott-Aldrich syndrome. *J Pediatr*. 1994;125:876-885.
- Derry JM, Ochs HD, Francke U. Isolation of a novel gene mutated in Wiskott-Aldrich syndrome. *Cell*. 1994;78:635-644.
- Devriendt K, Kim AS, Mathijs G, et al. Constitutively activating mutation in WASP causes X-linked severe congenital neutropenia. *Nat Genet*. 2001;27:313-317.
- Ancliff PJ, Blundell MP, Cory GO, et al. Two novel activating mutations in the Wiskott-Aldrich syndrome protein result in congenital neutropenia. *Blood*. 2006;108:2182-2189.
- Emanuel PD. Juvenile myelomonocytic leukemia. *Curr Hematol Rep*. 2004;3:203-209.
- Niemeyer CM, Arico M, Basso G, et al. Chronic myelomonocytic leukemia in childhood: a report of 110 cases. *Blood*. 1997;89:3534-3543.
- Niemeyer CM, Fenu S, Hasle H, et al. Differentiating juvenile myelomonocytic leukemia from infectious disease (letter). *Blood*. 1998;91:365-367.
- Tartaglia M, Niemeyer CM, Song X, et al. Somatic *PTPN11* mutations in juvenile myelomonocytic leukemia, myelodysplastic syndromes and acute myeloid leukemia. *Nat Genet*. 2003;34:148-150.
- Flotho C, Valcamonica S, Mach-Pascuala S, et al. Ras mutations and clonality analysis in children with juvenile myelomonocytic leukemia (JMML). *Leukemia*. 1999;13:32-37.
- Le DT, Kong N, Zhu Y, et al. Somatic inactivation of *Nf1* in hematopoietic cells results in a progressive myeloproliferative disorder. *Blood*. 2004;103:4243-4250.
- Yamamoto T, Isomura M, Xu Y, et al. *PTPN11*, *RAS* and *FLT3* mutations in childhood acute lymphoblastic leukemia. *Leuk Res*. 2006;30:1085-1089.
- Yamada M, Ariga T, Kawamura N, et al. Determination of carrier status for the Wiskott-Aldrich syndrome by flow cytometric analysis of Wiskott-Aldrich syndrome protein expression in peripheral blood mononuclear cells. *J Immunol*. 2000;165:1119-1122.
- Imai K, Morio T, Zhu Y, et al. Clinical course of patients with WASP gene mutations. *Blood*. 2004;103:456-464.
- Kajiwaru M, Nonoyama S, Eguchi M, et al. WASP is involved in proliferation and differentiation of human haemopoietic progenitors in vitro. *Br J Haematol*. 1999;107:254-262.
- Burns S, Cory GO, Vainchenker W, et al. Mechanisms of WASP-mediated hematologic and immunologic disease. *Blood*. 2004;104:3454-3462.
- Manabe A, Yoshimasu T, Ebihara Y, et al. Viral infections in juvenile myelomonocytic leukemia: prevalence and clinical implications. *J Pediatr Hematol Oncol*. 2004;26:636-641.
- Kirby MA, Weitzman S, Freedman MH. Juvenile chronic myelogenous leukemia: differentiation from infantile cytomegalovirus infection. *Am J Pediatr Hematol Oncol*. 1990;12:292-296.
- Herrod HG, Dow LW, Sullivan JL. Persistent Epstein-Barr virus infection mimicking juvenile chronic myelogenous leukemia: immunologic and hematologic studies. *Blood*. 1983;61:1098-1104.
- Yetgin S, Cetin M, Yenicesu I, et al. Acute parvovirus B19 infection mimicking juvenile myelomonocytic leukemia. *Eur J Haematol*. 2000;65:276-278.
- Kuijpers TW, van Bruggen R, Kamerbeek N, et al. Natural history and early diagnosis of LAD-1/variant syndrome. *Blood*. 2007;109:3529-3537.

LETTERS

Dominant-negative mutations in the DNA-binding domain of STAT3 cause hyper-IgE syndrome

Yoshiyuki Minegishi¹, Masako Saito¹, Shigeru Tsuchiya², Ikuya Tsuge³, Hidetoshi Takada⁴, Toshiro Hara⁴, Nobuaki Kawamura⁵, Tadashi Ariga⁵, Srdjan Pasic⁶, Oliver Stojkovic⁷, Ayse Metin⁸ & Hajime Karasuyama¹

Hyper-immunoglobulin E syndrome (HIES) is a compound primary immunodeficiency characterized by a highly elevated serum IgE, recurrent staphylococcal skin abscesses and cyst-forming pneumonia, with disproportionately milder inflammatory responses, referred to as cold abscesses, and skeletal abnormalities¹. Although some cases of familial HIES with autosomal dominant or recessive inheritance have been reported, most cases of HIES are sporadic, and their pathogenesis has remained mysterious for a long time. Here we show that dominant-negative mutations in the human signal transducer and activator of transcription 3 (STAT3) gene result in the classical multisystem HIES. We found that eight out of fifteen unrelated non-familial HIES patients had heterozygous STAT3 mutations, but their parents and siblings did not have the mutant STAT3 alleles, suggesting that these were *de novo* mutations. Five different mutations were found, all of which were located in the STAT3 DNA-binding domain. The patients' peripheral blood cells showed defective responses to cytokines, including interleukin (IL)-6 and IL-10, and the DNA-binding ability of STAT3 in these cells was greatly diminished. All five mutants were non-functional by themselves and showed dominant-negative effects when co-expressed with wild-type STAT3. These results highlight the multiple roles played by STAT3 in humans, and underline the critical involvement of multiple cytokine pathways in the pathogenesis of HIES.

Elevated serum IgE is a hallmark of many allergic disorders². Curiously enough, the hyper-IgE state is also observed in some primary immunodeficiency disorders, such as HIES, Wiskott-Aldrich syndrome, Omenn syndrome and Comèl-Netherton syndrome³. HIES (OMIM number 243700) was first reported in 1966 as Job's syndrome (OMIM number 147060)^{4,5}, but its underlying cause is still unknown, unlike the other three syndromes. In most cases of HIES, the clinical manifestations extend over multiple systems in the body, including the immune system, skeletal/dental system and soft tissue⁶. In contrast, the abnormalities in familial autosomal recessive (AR)-HIES patients seem to be confined to the immune system⁷. We previously identified a homozygous mutation of the tyrosine kinase 2 (TYK2) gene in a patient who showed AR-HIES and susceptibility to intracellular bacterial infections⁸. TYK2 is a non-receptor tyrosine kinase belonging to the JAK family^{9,10}. The patient's cells expressed no detectable TYK2 protein and displayed defects in multiple cytokine signals, including the signalling pathways for IL-6, IL-10, IL-12, IL-23 and type I IFN. The cytokine signals were successfully restored by introducing the intact TYK2 gene into the patient's cells. These multiple defects probably account for the patient's complex clinical manifestations⁸. The identification of a TYK2 deficiency in this HIES

patient indicated to us that, besides TYK2, one or more molecules shared by multiple cytokine signalling pathways might also cause HIES.

To explore this possibility, we first examined the responses to IL-6, IL-10, IL-12 and IFN α of peripheral blood cells from two patients (patient 1 and patient 2) who showed characteristics of multisystem HIES, including skeletal/dental abnormalities, skin abscesses, cyst-forming pneumonia and highly elevated serum IgE (Supplementary Table 1). The patients' B cells secreted IgM normally when stimulated with Epstein-Barr virus (EBV) infection (Fig. 1a). However, additional stimulation with IL-6 induced no significant increase in IgM secretion in the patients' B cells, unlike in the control B cells (Fig. 1a). Moreover, the suppression of lipopolysaccharide-induced production of TNF α by IL-10 deteriorated in the patients' macrophages (Fig. 1b). Thus, both the IL-6 and IL-10 pathways were defective in these HIES patients, as in the TYK2-deficient patient (Fig. 1a and 1b). In contrast, neither IL-12 nor IFN α signalling was impaired in the HIES patients, unlike in the TYK2-deficient patient (Fig. 1c and 1d). The HIES patients' T cells produced IFN γ normally in response to IL-12 (Fig. 1c), and their peripheral blood mononuclear cells (PBMCs) showed normal upregulation of transcripts for two IFN-inducible genes, *NMI* and *MX1* (also known as *MxA*), in response to IFN α (Fig. 1d). These observations indicated a possible abnormality in one or more molecules that was shared by the IL-6 and IL-10 signals but not essential for the IL-12 and IFN α pathways.

An array of cytokine signals is transduced by different combinations of JAK family kinases and STATs^{9,10}. When cytokines bind to their receptors, receptor-associated JAKs are activated to phosphorylate STATs, which in turn dimerize and translocate to the nucleus, where they activate target genes. In a survey of possible abnormalities in this signal cascade, we identified heterozygous mutations in the STAT3 DNA-binding domain in both patients: a single amino acid deletion (Δ V463) in patient 1 and a mis-sense mutation (R382W) in patient 2 (Fig. 2). Because STAT3 is shown to be activated in response to a wide variety of cytokines, growth factors, and hormones^{11,12}, we thought that its mutation could well account for the patients' complex clinical manifestations extending over multiple systems. Further analysis of the STAT3 complementary DNA sequences in thirteen more unrelated patients with non-familial HIES identified heterozygous mutations in six of these patients (patients 3–8; see Supplementary Table 1 for clinical summary), and all of these mutations were located in the DNA-binding domain of STAT3: Δ V463 in patient 3 and patient 8, like in patient 1; R382Q in patient 4; H437Y in patient 5; T389I in patient 6; R382W in patient 7, like in patient 2 (Fig. 2). The five different STAT3 mutations found in the

¹Department of Immune Regulation, Tokyo Medical and Dental University Graduate School, Tokyo 113-8519, Japan. ²Department of Pediatrics, Tohoku University Graduate School of Medicine, Sendai 980-8575, Japan. ³Department of Pediatrics, Fujita Health University, Aichi 470-1192, Japan. ⁴Department of Pediatrics, Kyushu University, Fukuoka 812-8582, Japan. ⁵Department of Pediatrics, Hokkaido University Graduate School of Medicine, Sapporo 060-8638, Japan. ⁶Pediatric Immunology, Mother and Child Health Institute, Belgrade 110 70, Serbia. ⁷Laboratory for Forensic Genetics, Institute of Forensic Medicine, University of Belgrade, Belgrade 110 70, Serbia. ⁸Pediatric Immunology Department, SB Ankara Diskapi Children's Hospital, Ankara 06110, Turkey.

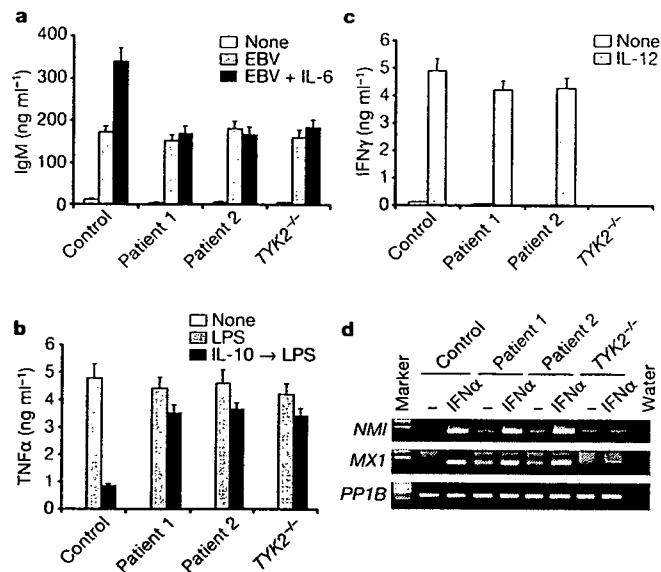


Figure 1 | Impaired responses to IL-6 and IL-10 in HIES patients' cells. **a**, IgM levels in culture medium of PBMCs from a control subject, two HIES patients (patient 1 and patient 2), and the TYK2-deficient patient, cultured for 7 days without stimulation, with EBV alone or with EBV and IL-6. **b**, TNF α levels in culture medium of macrophages from the same subjects, cultured without or with lipopolysaccharide (LPS) stimulation for 48 h, or with IL-10 treatment for 24 h before lipopolysaccharide stimulation. **c**, IFN γ in culture medium of CD4⁺ T cells from the same subjects, cultured for 24 h without or with IL-12. Error bars show standard deviations (**a–c**). **d**, *NMI*, *MX1* and cyclophilin B (*PP1B*) transcript levels in PBMCs from the same subjects were unstimulated or stimulated with IFN α for 2 h.

eight patients were all confirmed by sequencing their genomic DNA, and no sequence alterations were detected in any other parts of *STAT3*, *TYK2* or *JAK1*. The DNA-binding domain of STAT3 is highly conserved among different species in its amino acid sequence, and the alterations identified in the patients' *STAT3* gene were statistically highly significant in population genetics ($P < 10^{-15}$, Fisher's exact probability test), as judged by the fact that such alterations were not found in 1,000 unrelated healthy individuals analysed, including at least 100 controls from the patients' ethnic group. *STAT3* is located

on human chromosome 17q21, but not 4q, which was reported to contain a disease locus for familial AD-HIES¹⁵. None of the eight HIES patients in the present study had a known family history of HIES, and no mutation was detected in the *STAT3* cDNAs from all the parents and seven siblings of the patients, even though an analysis of multiple polymorphic markers confirmed the biological parent-child relationship (data not shown). Therefore, the mutations are likely to have occurred *de novo* in the HIES patients.

We next evaluated the biological significance of the *STAT3* mutations. The *STAT3* protein levels were comparable in all the EBV-transformed B-cell lines established from patients 1–6 and a control subject, and the extent of the tyrosine phosphorylation on *STAT3* induced by IFN α stimulation was also comparable (Fig. 3a). Furthermore, all the mutant proteins formed a complex with wild-type *STAT3* as efficiently as did wild-type *STAT3*, as judged by the co-immunoprecipitation of wild-type and mutant *STAT3* proteins co-expressed in COS7 cells (Fig. 3b). However, nuclear extracts isolated from the patients' cells stimulated with IFN α contained much lower amounts of active *STAT3* that could bind to target DNA compared with nuclear extracts from the control cells, whereas the DNA-binding activity of *STAT1* was intact in the patients' cells (Fig. 3c). This finding was consistent with a previous report showing that changing codons 461 to 463 in *STAT3* from Val-Val-Val to Ala-Ala-Ala resulted in the impairment of *STAT3*'s DNA-binding activity¹⁴. Thus, the genetic mutations identified in the HIES patients seemed to result in the impairment of the DNA-binding activity of *STAT3* and most likely that of heterodimers between mutant and wild-type *STAT3* molecules. A similar impairment of DNA-binding activity in *STAT1* protein was recently reported in cells isolated from patients carrying a heterozygous mutation in the DNA-binding domain of *STAT1* (ref. 15).

When wild-type *STAT3* was exogenously expressed—together with a luciferase reporter gene containing *STAT3*-responsive elements—in human HeLa cells in which the endogenous *STAT3* was knocked down, fivefold upregulation of luciferase activity in response to IFN α was detected (Fig. 4a). In contrast, none of the *STAT3* mutants conferred any significant increase of luciferase activity on the HeLa cells in response to IFN α , demonstrating a loss of function of the *STAT3* mutants. To explore the possibility that the *STAT3* mutant proteins function as dominant-negative, wild-type *STAT3* or the individual mutants were exogenously expressed in IL-6-responsive HepG2 cells and IL-10-responsive MC9 cells (Fig.

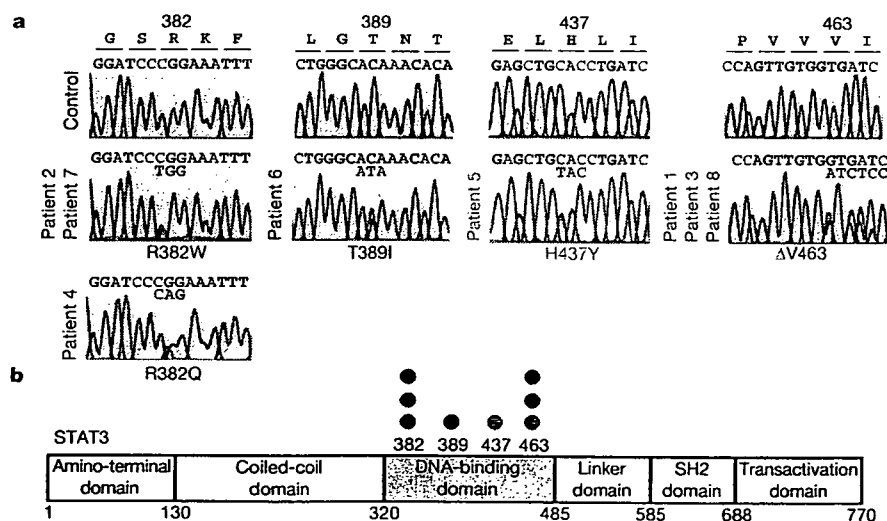


Figure 2 | Heterozygous mutations in the DNA-binding domain of *STAT3* from eight HIES patients. **a**, Electropherograms showing partial *STAT3* cDNA sequences from a control subject and the eight HIES patients. **b**, The

structure of *STAT3* is shown schematically, and the positions of the mutations identified in the eight patients are indicated.

4b and 4c). In HepG2 cells transfected with empty vector together with the reporter luciferase gene, the luciferase activity was upregulated as much as 3.5 times its basal level in response to IL-6 stimulation. The IL-6-induced upregulation of luciferase activity was augmented in HepG2 cells transfected with wild-type *STAT3* by up to 5.5 times, whereas it was severely impaired in cells transfected with any of the mutant *STAT3*s, showing at most a 2-fold increase (Fig. 4b). Moreover, the IL-10-induced downregulation of surface KIT (C-Kit) expression was severely impaired in MC/9 cells transfected with any of the mutant *STAT3*s, unlike those with empty vector or wild-type *STAT3* (Fig. 4c). Thus, all the *STAT3* mutants identified in the HIES patients displayed dominant-negative effects when co-expressed with wild-type *STAT3*.

The DNA-binding activity of *STAT3* in the IFN α -stimulated patients' cells was not totally abrogated, although it was only approximately one-fourth that of control cells (Fig. 3b). This residual *STAT3* activity might have rescued the patients from early embryonic death, which is observed in *STAT3*-deficient mice¹⁶. In contrast, its diminished activity might have an impact on the development and functions of multiple organ systems, leading to

compound clinical manifestations of HIES, given *STAT3*'s role in the signalling pathways of a variety of soluble factors, including the IL-6-family cytokines (IL-6, IL-11, IL-27, IL-31, LIF, OSM, CNTF and cardiotrophin-1), the IFN-family cytokines (IL-10, IL-19, IL-20, IL-22, IL-24, IL-26, IFN α/β and IFN γ), the IL-2-family cytokines (IL-2, IL-7, IL-9, IL-15 and IL-21), IL-5, IL-23, CSF3/G-CSF, EGF, CSF1 and leptin^{12,17,18}.

It has been shown that *STAT3* has important roles in the differentiation of both osteoblasts and osteoclasts *in vitro*¹⁹, and mice deficient for *STAT3* in osteoblasts show an osteoporotic phenotype²⁰. When osteoclasts were generated from peripheral blood monocytes in culture with CSF1/M-CSF and TNFSF11/RANKL, those from the HIES patients with the *STAT3* mutations showed higher bone-resorption activity compared to those from control subjects (Supplementary Fig. 1). This may reflect the skeletal/dental abnormalities

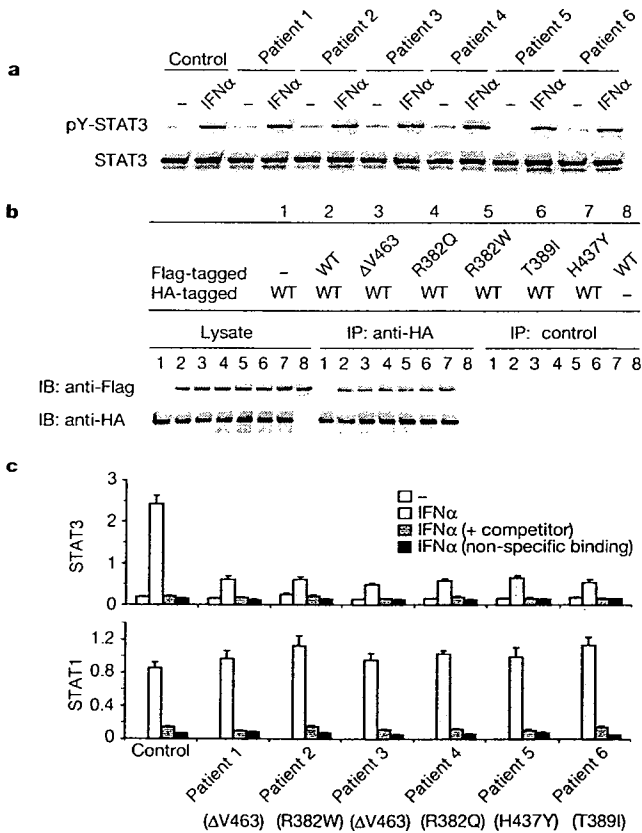


Figure 3 | Diminished DNA-binding activity of *STAT3* in the HIES patients' cells. **a**, Total and tyrosine-phosphorylated (pY-) *STAT3* proteins detected by immunoblotting. EBV-transformed B-cell lines (EBV-LCL) established from a control subject and the HIES patients were unstimulated or stimulated with IFN α for 15 min. **b**, Association of Flag- or HA-tagged wild-type (WT) and mutant *STAT3*s co-expressed in COS7 fibroblast cells was examined by immunoprecipitation (IP) with anti-HA or control antibody followed by immunoblotting (IB) with anti-Flag or HA antibody. **c**, DNA-binding activity of *STAT3* and *STAT1* in nuclear extracts prepared from EBV-LCLs from a healthy control and the HIES patients that were unstimulated or stimulated with IFN α for 15 min. Dark grey bars indicate the DNA-binding activity in the presence of competitor oligonucleotides, and black bars indicate non-specific binding to irrelevant oligonucleotides. Error bars are standard deviations.

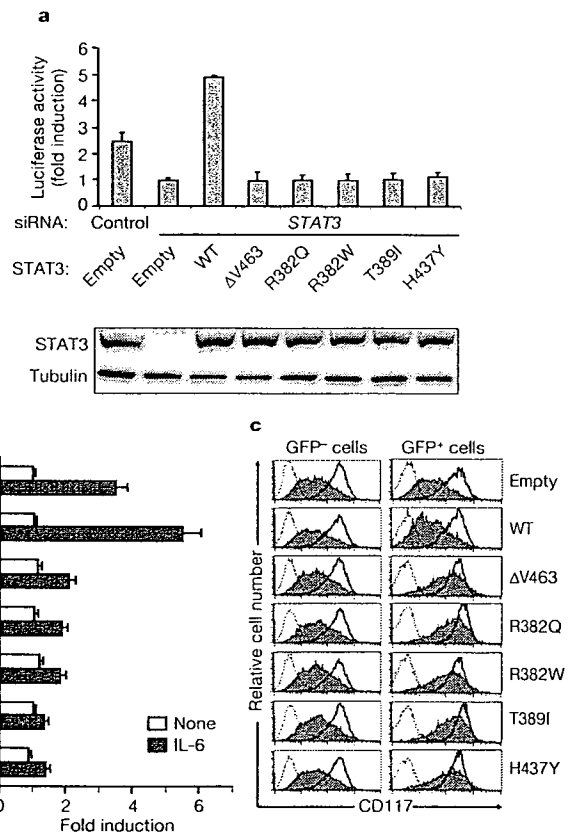


Figure 4 | Loss-of-function and dominant-negative effect of the *STAT3* mutants in cytokine signals. **a**, Wild-type or individual mutants of *STAT3* were exogenously expressed together with a luciferase reporter gene containing *STAT3*-responsive elements in human HeLa cells in which endogenous *STAT3* was knocked-down by transfecting with two sets of siRNA oligonucleotides. The HeLa cells were then left unstimulated or stimulated with 10 ng ml⁻¹ of IFN α for 5 h. The relative luciferase activity in the cell lysates of IFN α -stimulated versus unstimulated cells is shown (error bars show standard deviations). Expression of endogenous and exogenous *STAT3* proteins detected by immunoblotting is shown in the lower panel. **b**, The relative luciferase activity in the cell lysates of unstimulated or IL-6-stimulated HepG2 cells that were transfected with the luciferase reporter construct plus an empty vector or a vector containing the wild-type (WT) or one of each mutant *STAT3* sequence. Error bars show standard deviations. **c**, The CD117 expression level on untreated (thick line histograms) or IL-10-treated (shaded histograms) MC/9 cells that were infected with retroviral vectors containing WT or one of the mutant *STAT3* sequences. Data are shown for GFP⁺ infected and GFP⁻ uninfected cells, and thin dotted histograms indicate staining with a control antibody.

observed in HIES patients. Another remarkable feature of HIES is that patients are often afebrile and feel well¹, despite serious pneumonia or dermal pathology⁴. Indeed, acute-phase responses, such as an increase in serum C-reactive protein during severe infections, were diminished in our patients. STAT3 was originally identified as a protein binding to the IL-6-responsive element in the genes encoding hepatic acute-phase proteins^{21,22}, and the liver-specific inactivation of STAT3 leads to an impaired acute-phase response in mice²³. Thus, the apparent lack of classical inflammatory responses in HIES patients could be attributed to defective signalling of pro-inflammatory cytokines, including IL-6.

Enhanced IgE production in the patients may reflect dysregulated immune responses owing to the impaired response to IL-10, a critical negative regulator²⁴, even though the exact mechanism of hyper IgE remains to be determined, as in the case of other disorders such as Wiskott-Aldrich syndrome. HIES patients often suffer from severe staphylococcal infection in the skin and lung. STAT3 plays a critical part in T_H17 development²⁵, and IL-17 produced by T_H17 cells is protective in the host defence against extracellular bacteria²⁶. IL-22 stimulates cells in the skin and respiratory systems to produce β -defensins through STAT3 activation²⁷. Thus, the susceptibility to bacterial infection could be attributed, at least in part, to the defects in T_H17 development and IL-22 signalling. Among the 15 sporadic HIES patients investigated in this study, no apparent difference was observed in clinical phenotypes and severity between those with the STAT3 mutations and those without the mutations, indicating that other HIES aetiology might be functionally linked to STAT3.

In summary, the present study identified a human deficiency in STAT3 as a major cause of multisystem HIES. This study highlights the multiple and critical roles of STAT3 in humans. The identification of these STAT3 mutations as causative for HIES, in addition to the previous finding of a causative mutation in TYK2 (ref. 8), underlines the critical involvement of a variety of cytokine signals in the pathogenesis of HIES. The diagnosis of HIES early in life is often hampered by a paucity of specific clinical features. Our discovery of STAT3 as a major causative gene of this disease will facilitate earlier and definitive diagnosis, leading to the prevention of serious complications by prompting the start of prophylactic antibiotic treatment early in life.

METHODS SUMMARY

Patients. This study was approved by the institutional review board at the Tokyo Medical and Dental University; written informed consent was obtained from all the individuals studied. The clinical characteristics of the eight HIES patients investigated in this study are summarized in Supplementary Table 1, and all the patients display definitive phenotypes of multisystem HIES (score ≥ 40).

Stimulation of cells with cytokines, and measurement of cytokines and IgM production. Cells were stimulated for the indicated time in culture with cytokines as described previously⁸. The concentration of IFN γ and TNF α in the culture supernatants was determined by ELISA (BD-PharMingen), according to the manufacturer's instructions. The amount of IgM secretion from EBV-infected B cells was determined as previously described²⁸.

RT-PCR and direct sequence analysis. Extraction of total RNA, cDNA synthesis, PCR, semiquantitative RT-PCR, and sequencing were performed as previously described²⁹.

Immunoblotting and immunoprecipitation. Immunoblotting and immunoprecipitation were performed as described previously⁸.

Enzyme-linked DNA-protein interaction assay. Binding of STAT3 and STAT1 to their target DNA was measured using the Mercury TransFactor kit (Clontech Laboratories) according to the manufacturer's protocol.

Retroviral infections. Retroviral infections were done as described previously⁸.

Flow cytometric analysis. The surface immunophenotype was analysed as described³⁰.

STAT3 knock-down. Transfection of short interfering RNA (siRNA) oligonucleotides (5'-ccugcaagagucgaauguucuu-3' and 5'-gcaguucuuacagcag-guauuu-3') was performed as described previously⁸. Forty hours after transfection, the cells were treated with IFN α for 5 h. In the experiment shown

in Fig. 4a, nucleotide sequences of wild-type and mutant STAT3 cDNAs were modified so that they were insensitive to STAT3 siRNA, but they still encoded the original amino acid sequences of STAT3.

Luciferase reporter assay. The reporter construct of STAT3-responsive elements linked to a luciferase reporter gene was transfected with wild-type or mutant STAT3. Forty hours after the transfection, the cells were stimulated with 100 ng ml⁻¹ IL-6 for 5 h. Luciferase activity was measured with a dual-luciferase assay system according to the manufacturer's protocol (Promega).

Full Methods and any associated references are available in the online version of the paper at www.nature.com/nature.

Received 28 June; accepted 19 July 2007.

Published online 5 August 2007; corrected 30 August 2007 (details online).

- Grimbacher, B., Holland, S. M. & Puck, J. M. Hyper-IgE syndromes. *Immunol. Rev.* 203, 244–250 (2005).
- Gould, H. J. *et al.* The biology of IGE and the basis of allergic disease. *Annu. Rev. Immunol.* 21, 579–628 (2003).
- Grimbacher, B., Belohradsky, B. H. & Holland, S. M. Immunoglobulin E in primary immunodeficiency diseases. *Allergy* 57, 995–1007 (2002).
- Davis, S. D., Schaller, J. & Wedgwood, R. J. Job's Syndrome. Recurrent, "cold", staphylococcal abscesses. *Lancet* 1, 1013–1015 (1966).
- Buckley, R. H., Wray, B. B. & Belmaker, E. Z. Extreme hyperimmunoglobulinemia E and undue susceptibility to infection. *Pediatrics* 49, 59–70 (1972).
- Grimbacher, B. *et al.* Hyper-IgE syndrome with recurrent infections—an autosomal dominant multisystem disorder. *N. Engl. J. Med.* 340, 692–702 (1999).
- Renner, E. D. *et al.* Autosomal recessive hyperimmunoglobulin E syndrome: a distinct disease entity. *J. Pediatr.* 144, 93–99 (2004).
- Minegishi, Y. *et al.* Human tyrosine kinase 2 deficiency reveals its requisite roles in multiple cytokine signals involved in innate and acquired immunity. *Immunity* 25, 745–755 (2006).
- Schindler, C. & Darnell, J. E. Jr. Transcriptional responses to polypeptide ligands: the JAK-STAT pathway. *Annu. Rev. Biochem.* 64, 621–651 (1995).
- Ihle, J. N. Cytokine receptor signalling. *Nature* 377, 591–594 (1995).
- Levy, D. E. & Darnell, J. E. Jr. STATs: transcriptional control and biological impact. *Nature Rev. Mol. Cell Biol.* 3, 651–662 (2002).
- Kisseleva, T., Bhattacharya, S., Braunstein, J. & Schindler, C. W. Signaling through the JAK/STAT pathway, recent advances and future challenges. *Gene* 285, 1–24 (2002).
- Grimbacher, B. *et al.* Genetic linkage of hyper-IgE syndrome to chromosome 4. *Am. J. Hum. Genet.* 65, 735–744 (1999).
- Horvath, C. M., Wen, Z. & Darnell, J. E. Jr. A STAT protein domain that determines DNA sequence recognition suggests a novel DNA-binding domain. *Genes Dev.* 9, 984–994 (1995).
- Chappier, A. *et al.* Novel STAT1 alleles in otherwise healthy patients with mycobacterial disease. *PLoS Genet.* 2, e131 (2006).
- Takeda, K. *et al.* Targeted disruption of the mouse Stat3 gene leads to early embryonic lethality. *Proc. Natl Acad. Sci. USA* 94, 3801–3804 (1997).
- Darnell, J. E. Jr. STATs and gene regulation. *Science* 277, 1630–1635 (1997).
- Levy, D. E. & Lee, C. K. What does Stat3 do? *J. Clin. Invest.* 109, 1143–1148 (2002).
- O'Brien, C. A., Gubrij, I., Lin, S. C., Saylor, R. L. & Manolagas, S. C. STAT3 activation in stromal/osteoblastic cells is required for induction of the receptor activator of NF- κ B ligand and stimulation of osteoclastogenesis by gp130-utilizing cytokines or interleukin-1 but not 1,25-dihydroxyvitamin D3 or parathyroid hormone. *J. Biol. Chem.* 274, 19301–19308 (1999).
- Itoh, S. *et al.* A critical role for interleukin-6 family-mediated Stat3 activation in osteoblast differentiation and bone formation. *Bone* 39, 505–512 (2006).
- Akira, S. *et al.* Molecular cloning of APRF, a novel IFN-stimulated gene factor 3 p91-related transcription factor involved in the gp130-mediated signaling pathway. *Cell* 77, 63–71 (1994).
- Zhong, Z., Wen, Z. & Darnell, J. E. Jr. Stat3: a STAT family member activated by tyrosine phosphorylation in response to epidermal growth factor and interleukin-6. *Science* 264, 95–98 (1994).
- Li, W., Liang, X., Kellendonk, C., Poli, V. & Taub, R. STAT3 contributes to the mitogenic response of hepatocytes during liver regeneration. *J. Biol. Chem.* 277, 28411–28417 (2002).
- Robinson, D. S., Larche, M. & Durham, S. R. Tregs and allergic disease. *J. Clin. Invest.* 114, 1389–1397 (2004).
- Yang, X. O. *et al.* STAT3 regulates cytokine-mediated generation of inflammatory helper T cells. *J. Biol. Chem.* 282, 9358–9363 (2007).
- Happel, K. I. *et al.* Divergent roles of IL-23 and IL-12 in host defense against *Klebsiella pneumoniae*. *J. Exp. Med.* 202, 761–769 (2005).
- Wolk, K. *et al.* IL-22 increases the innate immunity of tissues. *Immunity* 21, 241–254 (2004).

28. Minegishi, Y. & Conley, M. E. Negative selection at the pre-BCR checkpoint elicited by human μ heavy chains with unusual CDR3 regions. *Immunity* 14, 631–641 (2001).
29. Minegishi, Y. *et al.* Mutations in Ig α (CD79a) result in a complete block in B-cell development. *J. Clin. Invest.* 104, 1115–1121 (1999).
30. Minegishi, Y. *et al.* An essential role for BLNK in human B cell development. *Science* 286, 1954–1957 (1999).

Supplementary Information is linked to the online version of the paper at www.nature.com/nature.

Acknowledgements We appreciate the willingness of the patients and the families to participate in this research study. This work is supported by the Japanese

Ministry of Education, Culture, Sports, Science and Technology, and the Japanese Ministry of Health, Labor and Welfare.

Author Contributions Y.M. designed and conducted most of the experiments; M.S. conducted the genetic analysis and the generation of osteoclasts; S.T., I.T., H.T., T.H., N.K., T.A., S.P. and A.M. diagnosed and collected samples; O.S. collected samples; H.K. oversaw the entire project; Y.M. and H.K. wrote the manuscript with comments from all co-authors.

Author Information Reprints and permissions information is available at www.nature.com/reprints. The authors declare no competing financial interests. Correspondence and requests for materials should be addressed to Y.M. (yminogishi.mbch@tmd.ac.jp).

METHODS

Patients. An immunological work-up revealed high serum IgE in all the patients and eosinophilia in five of them. All other laboratory data examined were within the normal range, including the lymphocyte subpopulations, their proliferative responses to mitogens, the levels and subclasses of serum immunoglobulins, the oxidative burst of granulocytes, and the number and size of platelets.

Antibodies and cytokines. Antibodies against STAT3, tyrosine-phosphorylated STAT3, Flag and HA, and HRP-conjugated rabbit anti-mouse and goat anti-rabbit antibodies were purchased from Cell Signaling. The CD117 monoclonal antibody was from BD-PharMingen, and the CD3 monoclonal antibody (OKT3) was from Janssen Pharmaceutical. Recombinant human IL-6, IL-10, IL-12, IFN α , and GM-CSF were purchased from Peprotech, recombinant human IL-2 from Shionogi, and lipopolysaccharide (055:B5) from Sigma-Aldrich.

Isolation and culture of T cells and macrophages from PBMCs. Isolation and cell culture of T cells and macrophages were performed as described previously⁸. All the experiments were performed at least three times with three different controls.

Stimulation of cells with cytokines, and measurement of cytokines and IgM production. Cells were stimulated for the indicated time in culture with IL-6 (100 ng ml⁻¹), IL-10 (100 ng ml⁻¹), IL-12 (10 ng ml⁻¹), or IFN α (5 ng ml⁻¹) as described previously⁸.

RT-PCR and direct sequence analysis. Sequencing was performed with an ABI Prism dRhodamine Terminator kit and analysed with an ABI Prism 310 DNA Sequencer (Perkin-Elmer Applied Biosystems). At least two independent PCR products were sequenced.

Enzyme-linked DNA-protein interaction assay. Thirty micrograms of nuclear extracts were incubated in a 96-well microplate precoated with oligonucleotides encoding the consensus binding sequence for STAT1 or that for STAT3. Bound STAT3 or STAT1 was detected with specific antibodies plus an HRP-conjugated secondary antibody.

Retroviral infections. Retroviral infections were done with the retroviral vector pMX-IRES-GFP (a gift from T. Kitamura) carrying the wild-type or one of each mutant STAT3 sequence as described previously⁸.

STAT3 knock-down. Transfection of siRNA oligonucleotides was performed by using Lipofectamine-RNAiMAX reagent (Invitrogen). Forty hours after transfection, the cells were treated with IFN α (10 ng ml⁻¹) for 5 h.

Luciferase reporter assay. The reporter construct contained 4 repeated STAT3-responsive elements linked to a luciferase reporter gene. HeLa cells or HepG2 cells were transfected with the pcDNA3 vector bearing wild-type or mutant STAT3, the reporter construct, and an expression vector for *Renilla* luciferase driven by the CMV reporter, with FuGENE6 (Roche). The relative luciferase activity was determined by normalizing the values against the *Renilla* luciferase signal.

STEM CELLS[®]

EMBRYONIC STEM CELLS

Genetically Manipulated Human Embryonic Stem Cell-derived Dendritic Cells with Immune Regulatory Function

Satoru Senju^a, Hirofumi Suemori^b, Hitoshi Zembutsu^c, Yasushi Uemura^a, Shinya Hirata^a, Daiki Fukuma^a, Hidetake Matsuyoshi^a, Manami Shimomura^a, Miwa Haruta^a, Satoshi Fukushima^a, Yusuke Matsunaga^a, Toyomasa Katagiri^c, Yusuke Nakamura^c, Masataka Furuya^b, Norio Nakatsuji^d, and Yasuharu Nishimura^a

^aThe Department of Immunogenetics, Graduate School of Medical Sciences, Kumamoto University, Kumamoto, Japan; ^bLaboratory of Embryonic Stem Cell Research, Stem Cell Research Center, Institute for Frontier Medical Sciences, Kyoto University, Kyoto, Japan; ^cLaboratory of Molecular Medicine, Human Genome Center, Institute of Medical Science, University of Tokyo, Tokyo, Japan; ^dDepartment of Development and Differentiation, Institute for Frontier Medical Sciences, Kyoto University, Kyoto, Japan

Key Words. Dendritic Cells • Embryonic Stem Cells • Cell Differentiation • Cell Therapy

ABSTRACT

Genetically manipulated dendritic cells (DC) are considered to be a promising means for antigen-specific immune therapy. This study reports generation, characterization, and genetic modification of dendritic cells (DC) derived from human embryonic stem (ES) cells. The human ES cell-derived DC (ES-DC) expressed surface molecules typically expressed by DC, and had capacities to stimulate allogeneic T lymphocytes and to process and present protein antigen in the context of HLA class II molecule. Genetic modification of human ES-DC can be accomplished without the use of viral vectors, by the introduction of expression vector plasmids into undifferentiated ES cells by electroporation and subsequent induction of differentiation of the

transfectant ES cell clones to ES-DC. ES-DC introduced with invariant chain-based antigen-presenting vectors by this procedure stimulated HLA-DR-restricted antigen-specific T cells in the absence of exogenous antigen. Forced expression of PD-L1 in ES-DC resulted in the reduction of the proliferative response of allogeneic T cells co-cultured with the ES-DC. Generation and genetic modification of ES-DC from non-human primate, cynomolgus monkey, ES cells was also achieved by the currently established method. ES-DC technology is therefore considered to be a novel means for immune therapy.

Corresponding Author: Satoru Senju, Department of Immunogenetics, Graduate School of Medical Sciences, Kumamoto University, 1-1-1 Honjo, Kumamoto 860-8556, Japan, Fax: +81-96-373-5314, e-mail: senjusat@gpo.kumamoto-u.ac.jp, Grant Support: Supported in part by Grants-in-Aid 12213111, 14657082, 14570421, 14370115, 16590988, 17390292, 17015035 and 18014023 from the Ministry of Education, Science, Technology, Sports, and Culture (MEXT), Japan, the Program of Founding Research Centers for Emerging and Reemerging Infectious Diseases launched as a project commissioned by MEXT, Japan, Research Grant for Intractable Diseases from Ministry of Health and Welfare, Japan, Oncotherapy Science Inc. (to Ya.Ni.), and grants from Japan Science and Technology Agency (JST), the Tokyo Biochemical Research Foundation, Uehara Memorial Foundation, and Takeda Science Foundation.; Received April 30, 2007; accepted for publication July 27, 2007; first published online in Stem Cells Express August 9, 2007. ©AlphaMed Press 1066-5099/2007/\$30.00/0 doi: 10.1634/stemcells.2007-0321, Received April 30, 2007; accepted for publication July 27, 2007; first published online in Stem Cells Express August 9, 2007. ©AlphaMed Press 1066-5099/2007/\$30.00/0 doi: 10.1634/stemcells.2007-0321

INTRODUCTION

Embryonic stem (ES) cells are characterized by pluripotency and infinite propagation capacity, and the methods for genetic modification of ES cells including targeted gene modification have been well established. This laboratory and others have devised methods to generate dendritic cells (DC) *in vitro* from mouse ES cells [1, 2]. The functions of mouse ES cell-derived DC (esDC or ES-DC), including stimulation of allogeneic T cells, processing and presentation of antigenic proteins, and migration upon *in vivo* transfer, were comparable to those of DC generated *in vitro* from bone marrow cells [3]. This laboratory has also established a strategy for the genetic modification of mouse ES-DC [1]. Expression vectors were introduced into ES cells by electroporation and subsequently the transfectant ES cell clones were induced to differentiate to ES-DC. The studies using mice have demonstrated that *in vivo* transfer of genetically engineered mouse ES-DC is very useful for modulation of immune responses both positively and negatively. It is possible to induce anti-cancer immunity [3-6] and prevent autoimmune disease [7, 8] in mouse models with genetically engineered ES-DC.

In the present study, looking toward the future clinical application of ES-DC technology, a method was developed to generate ES-DC from human ES cells. The morphology and the results of functional and flowcytometric analyses indicate that human ES-DC possess the characteristic features of DC. cDNA microarray analysis revealed that the change of gene expression profile during generation and maturation of human ES-DC mimics partially that of monocyte-derived DC (Mo-DC). The currently established method was also applicable to cynomolgus monkey (*Macaca fascicularis*) ES cells.

MATERIALS AND METHODS

Cell lines, cytokines, and reagents

The use of human ES cells was done in accordance with "The Guidelines for Derivation and Utilization of Human Embryonic Stem Cells (2001)" of the Ministry of Education, Culture, Sports, Science and Technology, Japan, after approval by the Institutional Review Board. The human ES cell lines, KhES-1 and KhES-3, were recently established and maintained on mouse primary embryonic fibroblast (PEF) feeder layers as previously described [9, 10]. Mouse-derived hematopoietic stromal cell line OP9 was treated with mitomycin C (10 μ g/ml) for 1 hour before plating onto gelatin-coated tissue culture dishes to make feeder cell layers. The establishment and maintenance of cynomolgus monkey ES cell line, CMK6, was also reported [11, 12]. Recombinant human granulocyte macrophage colony stimulating factor (GM-CSF), macrophage colony stimulating factor (M-CSF), interleukin-4 (IL-4), tumor necrosis factor (TNF)- α , and soluble CD40-ligand were purchased from Peptotec (London, UK). Lipopolysaccharide (LPS) from *E. coli* and OK-432 were purchased from Sigma Chemicals (St. Louis, MO) and Chugai Pharmaceutical (Tokyo, Japan), respectively.

Induction of differentiation of ES cells into ES-DC

The procedure for differentiation culture was composed of 3 steps (Figure 1A). Step 1: Undifferentiated ES cells maintained on PEF were rinsed with phosphate-buffered saline (PBS) and treated with dissociation solution, CTK [10], and cultured on OP9 feeder cell layers in minimum essential medium alpha (α -MEM) supplemented with 20% fetal calf serum (FCS) and 2-ME (50 μ M). Culture of cells was continued for 14-18 days with human ES cells and for 11-13 days with cynomolgus monkey ES

cells, and the medium was changed once every 3 days. At the end of this step, the cells were rinsed with PBS and treated with trypsin /EDTA (PBS containing 0.25% trypsin and 1 mM EDTA) for 30-40 min and recovered. After re-suspension in culture medium, the cells were plated onto culture dishes and incubated for 2-4 hours. Thereafter, floating or weakly adherent cells were recovered by pipetting, and any firmly adherent cells were discarded. Step 2: After passaged through nylon mesh (Cell Strainer 100 μ m, BD Falcon, Bedford, MA), cells recovered from one 90-mm dish were plated in two dishes with freshly prepared OP9 feeder layers. On the following day, the culture medium was exchanged with a medium containing GM-CSF (100 ng/ml) and M-CSF (50 ng/ml). The culture was continued for 7-10 days, depending on the propagation of floating cells on the feeder layers. Step 3: ES cell-derived floating cells were recovered by pipetting and re-suspended in RPMI-1640 medium containing 10% FCS, GM-CSF (100 ng/ml), and IL-4 (10 ng/ml), and cultured in Petri dishes ($3-5 \times 10^5$ cells/dish) without a feeder layer (Locus, Tokyo, Japan). To induce maturation, IL-4 (10 ng/ml), TNF- α (10 ng/ml), and lipopolysaccharide (LPS, 3 μ g/ml) and, in some experiments, soluble CD40-ligand (20 ng/ml) or OK-432 (10 μ g / ml) were simultaneously added on day 3 or 5 of this step, and the culture was continued for further 2-3 days. Differentiating cells were microscopically analyzed on an inverted microscope (IX70, Olympus, Tokyo, Japan).

Flowcytometric analysis

The following monoclonal Ab conjugated with fluorescein isothiocyanate or phycoerythrin were purchased from Pharmingen (San Diego, CA) or eBioscience (San Diego, CA): anti-human histocompatibility leukocyte antigen (HLA)-DR (clone L243, mouse IgG2a), anti-HLA-A, B, C (clone G46-2.6, mouse IgG1), anti-human CD80 (clone L307.4, mouse IgG1), anti-human CD83

(clone HB15e, mouse IgG1), anti-human CD86 (clone FUN-1, mouse IgG1), anti-human CD40 (clone 5C3, mouse IgG1), anti-human B7-H1/PD-L1 (clone MIH1, mouse IgG1), and anti-human CD74 (clone M-B741, mouse IgG2a). As isotype-matched controls, mouse IgG2a (clone G155-178) and mouse IgG1 (clone MOPC-21) were used. The cell samples were treated with FcR-blocking reagent (Miltenyi Biotec, Bergish-Gladbach, Germany) for 10 min, stained with the fluorochrome-conjugated Ab for 30 min, and washed 3 times with PBS/2% FCS. Intracellular staining with anti-CD74 mAb was done by using IntraPrep (Beckman Coulter, Marseille, France). Stained cell samples were analyzed on a FACScan flowcytometer, and, in some experiments, the DC fraction was gated by forward and side scatters.

ELISA to detect cytokine production by ES-DC

Cells were cultured in 96-well flat-bottomed culture plates (1.2×10^5 cells / 150 μ l medium / well) in the presence or absence of soluble CD40-ligand, LPS, or OK432. After 60 hours of culture, supernatant was collected and concentration of TNF- α and IL-12 p70 was measured by using ELISA kits (Pierce, Rockford, IL).

Allogeneic T cell-stimulation assay

Mononuclear cells were isolated from heparinized peripheral blood of a human or a cynomolgus monkey housed in the Chemo-Sero-Therapeutic Research Institute (Kumamoto, Japan), using Ficoll-Paque PLUS (Amersham Biosciences, Uppsala, Sweden). T cells were purified using the Pan T cell isolation kit for humans or the kit for non-human primates (Miltenyi Biotec, Bergish-Gladbach, Germany). The T cells (4×10^4 /well) were co-cultured with graded numbers of X-ray irradiated (40 Gy) stimulator cells in RPMI-1640 medium supplemented with 10% human plasma in 96-

well round-bottomed culture plates for 5 days. [³H]-thymidine (247.9 Gbq/mmol) was added to the culture (0.037 Mbq/well) for the last 16 hours. At the end this time, the cells were harvested onto glass fiber filters (Wallac, Turku, Finland) and the incorporation of [³H]-thymidine was measured by scintillation counting. In the experiment using PD-L1-transfectant ES-DC, anti-PD-L1 blocking Ab (clone MIH1, eBioscience) or control mouse IgG1 Ab (eBioscience) was added to the culture (10 µg/ml).

Recombinant antigenic protein

A DNA fragment encoding human glutamic acid decarboxylase (GAD65) p96-174 protein fragment was cloned into the prokaryotic expression vector pGEX-4T-3 (Amersham), to generate a vector for glutathione-S-transferase-fused GAD65 protein fragment (GST-GAD). The induction of the production of recombinant protein in *Escherichia coli* (DH5α) and the extraction of the recombinant protein from bacterial inclusion bodies was done according to Frangioni and Neel [13]. The purification of the recombinant protein with glutathion-agarose (Sigma, St. Louis, MO) was done as described in our previous report [14, 15]. The purity and integrity of the recombinant protein was confirmed by sodium dodecyl sulfate-polyacrylamide gel electrophoresis. The protein was concentrated and separated from small peptide fragments, if any, with Centricon-10 (Millipore, Bedford, MA) and the solvent was changed from the elution buffer to the culture medium by dialysis.

Antigen presentation assay

A human CD4⁺ T cell clone, SA32.5, recognizing GAD65p111-131 in the context of HLA-DR53 molecule (DRA*0101+DRB4*0103) was established and maintained, as previously described [16]. In the assay with the synthetic peptide, ES-DC

stimulated with TNF-α (10 ng/ml) plus LPS (3 µg/ml) were harvested, incubated in the presence of peptide (6 µM) for 3 hours, washed 4 times with culture medium, and X-ray irradiated (35 Gy). A T cell proliferation assay was set up in a 96-well flat-bottomed culture plate with SA32.5 T cells (3 x 10⁴ / well) and graded numbers of the peptide-loaded ES-DC in RPMI-1640 medium supplemented with 10% human plasma. In the assay with recombinant protein, the indicated amount of GST or GST-GAD protein was added to the co-culture of SA32.5 T cells (3 x 10⁴ / well) and irradiated ES-DC (1 x 10⁴ / well). After 48 hours of culture [³H]-thymidine was added, and then after an additional 16 hours of culture, the cells were harvested and the incorporated radioactivity was counted.

Plasmid construction

cDNA for human PD-L1 was isolated by PCR with Pyrobest DNA polymerase (Takara, Osaka, Japan) using cDNA clone CS0DI011 purchased from Invitrogen (Carlsbad, CA) as a template. Double-stranded oligo DNA (5'-atgaacattttacttcagtatgtggtgaaaagtttcgat-3') coding for GAD65p115-127 (the core epitope for SA32.5 T cell clone) was ligated to human invariant chain (Ii)-based epitope presentation vector pCI [17] to generate GAD65-epitope-fused Ii. A cDNA fragment for HLA-DRB4*0103 was generated by reverse transcriptase (RT)-PCR from RNA isolated from peripheral blood mononuclear cells positive for HLA-DRB4*0103. The coding DNA fragments were cloned into a mammalian expression vector, pCAG-IRES-Neo, which is driven by the CAG promoter and includes an internal ribosomal entry site (IRES)-neomycin-resistance gene cassette [3].

Transfection of ES cells

Human ES cells were harvested using CTK solution, dissociated into clusters of 50-100 cells by pipetting, and washed twice with Dulbecco

MEM (DMEM). The cells harvested from two 90-mm culture dishes with sub-confluently growing ES cells were suspended in 0.1 ml of DMEM and mixed with 50 μ g of linearized plasmid DNA dissolved in 0.1 ml of PBS in a 4 mm-gap cuvette. The electroporation of human ES cells was performed at 150 V and 200 μ F on Gene Pulsar (Bio-Rad, Hercules, CA). The transfection of cynomolgus monkey ES cells was done as previously described [18], with some modifications. Cynomolgus monkey ES cells were harvested after treatment with trypsin-EDTA. 1-1.5 $\times 10^7$ ES cells suspended in 0.7 ml of DMEM were mixed with 50 μ g of plasmid DNA in 0.1 ml of PBS in a 4 mm-gap cuvette. Electroporation was done at 250 V and 500 μ F. After electroporation, the ES cells were cultured on G418-resistant PEF feeder layers in 90-mm culture dishes or 6-well plates. Selection with G418 (150 μ g/ml) was done from 2-4 days after the transfection and G418-resistant ES cell colonies were picked up using a micropipette under microscopic observation on days 15-18 for human ES cells and on day 11 for monkey ES cells. The transfectant clones were transferred to 24-well culture plates with PEF and expanded in the presence of G418. ES cell transfectant clones with relatively high levels of expression of the transgene were selected based on the resistance to high dose (1-3 mg/ml) of G418 and also on the results of the RT-PCR analysis. Thereafter, the clones were subjected to the differentiation procedures. At the proper stages of differentiation, the cells were screened to select ES cell clones which highly expressed the transgene after differentiation, based on a flowcytometric analysis for PD-L1 and Ii transfectant human ES cells and on the antigen-presenting capacity for HLA-DRB4 transfectant cynomolgus monkey ES cells.

RT-PCR for detection of the transgene-derived transcripts

cDNA was synthesized from total cellular RNA with random hexamer primers and Superscript II reverse transcriptase (Invitrogen). The following PCR primer sets were used: 5'-gctggattacatcaagcactgaa-3' and 5'-caacaaagtctggcttatatccaa-3' for hypoxanthine guanine phosphoribosil transferase (HPRT) and 5'-ctgactgaccgcgttactcccaca-3' and 5'-ttggtatagatgtatctgacaggt-3' for transgene-derived DRB4 transcript.

RESULTS

Differentiation of human ES cells to ES-DC

Based on previous experience in the generation of dendritic cells from mouse ES cells [1] and also based on the findings in a preliminary study using cynomolgus monkey ES cells, feeder cell-culture method was adopted for the generation of dendritic cells from human ES cells, instead of the embryoid body (EB)-based method. The human ES cell line selected was KhES-1 which exhibited the highest growth rate among the 3 lines of human ES cell lines established in a recent study [9, 19]. For feeder cells, 3 lines of mouse stromal cell lines, ST2, OP9, and PA6 were evaluated for their capacity to induce hematopoietic differentiation of KhES-1 ES cells, and OP9 had the best yield among them (data not shown).

The protocol for the differentiation culture to generate ES-DC from human ES cells developed in the current study is composed of 3 steps, as shown in Figure 1A. At the beginning of the differentiation culture, undifferentiated ES cells maintained on mouse PEF feeders (Fig. 1B) were harvested using dissociation solution, CTK [9], and plated on OP9 feeder cell layers (step 1). Next, the ES cells grew and formed clusters composed mostly of epithelial cell-like large flat cells (Fig. 1C, D). Clusters of round, cobble

stone-like cells also appeared at about day 8, and those resembled the mesodermally differentiated cell clusters observed in hematopoietic differentiation culture of mouse ES cells [1, 20]. The size and number of round cell clusters gradually increased, and, around day 15, covered 20-30 % of the surface area (Fig. 1E).

On days 15-18 of the first step, cells were recovered from the dishes using trypsin/EDTA, and then isolated non-adherent cells were seeded onto freshly prepared OP9 cell layers, to begin the 2nd step. On the next day, the culture medium was exchanged for medium containing GM-CSF and M-CSF. Thereafter, small round cells, floating or loosely adhering to the feeder layer, appeared and gradually increased in number (Fig. 1F). The growth of the round cells depended primarily upon GM-CSF, thus suggesting that they grew in response to that factor. The cells were recovered and analyzed for their expression of hematopoietic cell lineage markers by flowcytometry (Fig. 2A). The cells expressed CD34 and CD45, and thus indicating that they followed a hematopoietic cell lineage. They also expressed CD31, CD43, and CD11b, thus collectively indicating a commitment to a myeloid cell lineage. The double peaks seen in the histograms in Figure 2 reflect the heterogeneity of the analyzed cells in size and intensity of autofluorescence.

On days 7-10 of the 2nd step, the floating or loosely adherent cells were harvested by pipetting and they were transferred to Petri dishes without feeder cells and cultured in the presence of GM-CSF and IL-4 (the 3rd step). Following this passage, the cells changed their morphology from round to irregular shape, and some had protrusions (Fig. 1G). Cells with protrusions gradually increased and more than 50% of the cells exhibited DC-like irregular shape after 2-3 days (Fig. 1H). The floating cells expressed CD86 and CD40, but scarcely

expressed CD80 and CD83 (Fig. 2B). Expression of HLA-DR at this stage differed between experiments.

Figures 1I and 1J show the cells after the simultaneous addition of TNF- α , LPS, soluble CD40-ligand, and IL-4. Generally they exhibited longer protrusions than before the stimulation and some of the protrusions were veil-like. Many of the cells formed aggregates. Flowcytometric analysis showed the increased expression of CD86 and the expression of CD80, CD83, and HLA-DR (Fig. 2B). Collectively, the cells exhibited the characteristics of DC in their morphology and expression of surface molecules, and thus they were designated as human ES-DC.

Production of IL-12 and TNF- α by ES-DC was measured by ELISA (Fig. 3). Production of TNF- α was profoundly induced by either LPS or OK432. OK432, but LPS did not, induced the production of IL-12, consistent with the reports that OK432 is an efficient inducer of IL-12 [21, 22]. Addition of CD40-ligand showed little effect on the production of these cytokines by human ES-DC.

ES-cell derived floating cells first appeared during the 2nd step of the culture for differentiation (pre-ES-DC) and could readily be isolated by pipetting procedure. Their morphology, pattern of expression of surface molecules, and T cell-stimulation capacity (described below) continuously changed until the final maturation. To determine the change in gene expression associated with such changes in the phenotypes, the gene expression profiles of pre-ES-DC, immature ES-DC, and mature ES-DC were analyzed using cDNA microarrays. For reference purposes, human peripheral blood monocytes and immature and mature monocyte-derived DC (Mo-DC) were also analyzed. The data for genes with relevance to immune

functions were selected from the total microarray data and are shown in supplemental Table I. Consistent with the results of flowcytometric analysis (Fig. 2B), up-regulation of the expression of genes encoding for cell surface molecules such as HLA class I, HLA class II, CD86 and CD40 along with differentiation of ES-DC was observed. In addition, expression of the genes related to DC function including CD74/invariant chain, CCR7, and CCL17/TARC was increased during the differentiation. Clustering analysis indicates similarity between change of the gene expression pattern from monocytes to immature Mo-DC and that from pre-ES-DC to immature ES-DC as well as that from immature Mo-DC to mature Mo-DC and that from immature ES-DC to mature ES-DC (supplemental Fig. 1).

The protocol of differentiation culture described to this point was originally developed using the KhES-1 line of human ES cells. This differentiation procedure was also applied to KhES-3, another human ES cell line. KhES-3 differentiation was similar to KhES-1 except that KhES-3 differentiated slightly more quickly than KhES-1, and a 1st step culture of 14-15 days was sufficient for the differentiation of KhES-3.

Function of human ES-DC

The capacity of the human ES-DC to stimulate T cells was examined based on the proliferative response of allogeneic T cells co-cultured with ES-DC (Fig. 4A). ES cell-derived floating cells recovered from the 2nd step (pre-ES-DC) showed little capacity to induce a response of T cells. In contrast, ES-DC following the 3rd step before the addition of maturation stimuli (immature ES-DC) showed a weak but definite stimulation, and following exposure to the maturation stimuli (mature ES-DC) showed a strong capacity to stimulate allogeneic T cells to proliferate.

Next, the antigen presenting capacity of ES-DC was examined. KhES-1 is positive for the HLA-DRB4*0103 gene encoding β chain of HLA-DR53 molecule. Presumably, ES-DC derived from KhES-1 should express the DR53 molecule, and their ability to present antigen to DR53-restricted CD4⁺ T cells was determined. As shown in Figure 4B, KhES-1-derived ES-DC pre-loaded with GAD65-derived synthetic peptide stimulated GAD65-specific DR53-restricted human T cell clone, SA32.5, to proliferate. To examine the capacity to process antigenic protein and present epitope, recombinant protein was used as the antigen (Fig. 4C). The SA32.5 T cell clone co-cultured with the ES-DC in the presence of recombinant GAD65 protein also showed proliferative response, thus indicating that ES-DC processed the antigenic protein and presented the epitope derived from the protein in the context of HLA class II molecules.

Genetic modification of human ES-DC

Previous research established a strategy for the genetic modification of mouse ES-DC [1]. Briefly, the expression vectors were introduced into ES cells by electroporation and subsequently the transfectant ES cell clones were induced to differentiate to ES-DC. The following experiments were performed to determine whether or not this strategy could be applicable to human ES cells.

PD-L1/B7-H1 is known to down-modulate responses of T cells upon interaction with the ligand, PD-1 on T cells [23]. An expression vector for human PD-L1 was introduced to KhES-1 by electroporation. The expression vector used was pCAG-Neo driven by the CAG promoter and containing an IRES-neomycin-resistance gene cassette (Fig. 5A). Among the transfectant clones, 23 ES cell clones showing resistance to high doses of G418 (2 mg/ml) were

selected and subjected to the ES-DC-differentiation culture.

The expression of PD-L1 of the transfectant clones was examined by a flowcytometric analysis at the stage of immature ES-DC, harvested on day 2 of the 3rd step of the differentiation culture. Although even non-transfectant ES-DC evidently expressed PD-L1 after maturation (data not shown), only a small population of them expressed PD-L1 at this stage (Fig. 5B, K1ES-DC). Based on the results of the analysis, one transfectant clone, KhES1-PD28, expressing the highest level of PD-L1 after the differentiation into immature ES-DC was selected (Fig. 5B). Allogeneic T cells co-cultured with immature ES-DC-PD28 showed significantly lower response than those co-cultured with non-transfectant immature ES-DC ($p < 0.05$, Fig. 5C). The proliferation-reducing effect of the transgene-derived PD-L1 was abrogated by the addition of anti-PD-L1 blocking Ab ($p < 0.01$), ruling out the possibility that the introduction of the PD-L1 expression vector impaired the differentiation of ES-DC. Collectively, these results suggest that forced expression of PD-L1 on ES-DC down-modulated the proliferative response of co-cultured allogeneic T cells via the interaction of PD-L1 with PD-1 on the T cells.

ES-DC carrying an epitope-presenting vector and expressing recombinant human invariant chain (Ii/CD74), which included GAD65p115-127 in the CLIP (class II-associated invariant chain peptide) region, were also generated (Fig. 5D). It was expected that the epitope could be efficiently targeted to MHC class II pathway [17]. Using a protocol similar to that used for the generation of PD-L1 transfectants, the vector was introduced into KhES-1 ES cells, and a transfectant clone, KhES-1-Ii23, highly expressing transgene-derived recombinant CD74 was selected by a flowcytometric analysis at the

pre-ES-DC stage. The expression of CD74 was detected even in the non-transfectant pre-ES-DC, reflecting intrinsic expression of CD74 (Fig. 5E). The transfectant exhibited an increased expression of CD74 in comparison to the non-transfectants, thus indicating additional expression of the molecule derived from the transgene. The ability of the transfectant ES-DC, ES-DC-Ii23 to stimulate the GAD-epitope specific T cell clone, SA32.5, in the absence of antigenic peptide or protein was next examined. As a result, ES-DC-Ii23 stimulated SA32.5 T cells and induced the proliferation of them, thus demonstrating functional expression of the epitope-presentation vector in the transfectant ES-DC (Fig. 5F). The *in vivo* transfer of ES-DC transfected with this antigen-presenting vector is therefore expected to be useful for controlling the immune response in an antigen specific manner [7].

Generation and genetic modification of cynomolgus monkey ES-DC

The differentiation protocol established using human ES cells was then applied to non-human primate ES cells. An ES cell line derived from cynomolgus monkey, CMK6 [11], was subjected to the ES-DC differentiation culture. Following the transfer to OP9 feeder layers, CMK6 cells grew and differentiated more rapidly than did human ES cells, KhES-1 and KhES-3. The optimal duration of the 1st step of the differentiation culture for CMK6 was 11-13 days, while the duration ranged 14-18 days for human ES cells. Figures 6A-C illustrate the morphological changes of CMK6-derived cells following the 2nd step of the differentiation culture. The surface phenotypes of the CMK6-derived pre-ES-DC, immature ES-DC, and mature ES-DC were then analyzed by flowcytometry (Fig. 6D). The double peaks seen in the histograms in Figure 6D reflect the heterogeneity of the analyzed cells in size and intensity of autofluorescence. Cynomolgus

monkey ES-DC had the capacity to stimulate allogeneic cynomolgus monkey T cells (Fig. 6E), as human ES-DC did.

The expression vector for HLA-DRB4*0103 (Fig. 7A) was introduced to CMK6. An analysis of the partial nucleotide sequence of DRA (CyLA-DRA) gene of CMK6 showed that the predicted amino acid sequence of CyLA-DR α chain is very similar to that of HLA-DR α with only one amino acid difference in α 1 domain (Genbank Accession AY591919). This suggested that the transgene-derived HLA-DR β chain could associate with the intrinsic CyLA-DR α chain expressed in cynomolgus ES-DC and present antigen to human T cells. The expression of the transgene before and after the ES-DC differentiation was confirmed by an RT-PCR analysis (Fig. 7B). ES-DC derived from a transfectant ES cell clone, cES-53-23, were pre-pulsed with synthetic GAD65 peptide and co-cultured with the HLA-DR53-restricted, GAD65-specific T cell clone, SA32.5. Figure 7C shows that the GAD65 peptide-pulsed transfectant ES-DC stimulated the T cells to proliferate. In contrast, ES-DC originating from parental ES cells pre-pulsed with the peptide could not stimulate the T cell clone. In addition, DR53-transfectant cynomolgus ES-DC had the capacity to process and present protein antigen to the T cells (Fig. 7D). These results demonstrate the antigen-processing and presenting capacity of cynomolgus ES-DC and also the functional expression of the transgene that had been introduced into the ES cells before the differentiation. Thus, the effect and safety of the immune therapy by the *in vivo* transfer of ES-DC can be examined by pre-clinical studies using cynomolgus monkeys.

DISCUSSION

To establish the current culture protocol, various culture conditions were tested. As feeder cell lines, 3 lines of mouse stromal cells, OP9, PA6, and ST2 were comparatively evaluated. As a result, the use of OP9 was thus observed to produce the highest yield of ES-DC. Although ST2 also worked as feeder cells in the 2nd step, the yield of ES-DC was about half of that in comparison to OP9. It was also essential to remove any firmly adherent cells, when transferring the cells from the 1st to 2nd step, by the procedure described in the Materials and Methods. At the end of the 1st step, many flat, adherent ES cell-derived cells were observed to form monolayers in the dishes. They probably differentiated into cell lineages other than mesoderm, and, unless removed, they grew rapidly in the 2nd step and inhibited the growth of hematopoietic cells.

Previously, two other groups reported the generation of functional antigen presenting cells or DC from human ES cells. Zhan et al. adapted embryoid body-based induction of hematopoietic differentiation [24]. Slukvin and colleagues recently reported a method using OP9 [25]. Although there are some similarities between Slukvin's method and the currently reported one, the two methods differ in the following points.

In both methods, human ES cells were co-cultured with OP9 feeder cells at the initial differentiation step (the 1st step). However, the duration of this culture step in our method (14-18 days) is significantly longer than 10 days of Slukvin's method. In our system, cells with morphology indicating mesodermal differentiation first appeared on day 8 or 9, and the extension of the 1st step culture to day 14-18 significantly improved the yield of hematopoietically differentiated cells (Fig. 1D, E). In addition, we pre-treated OP9 cells with

mitomycin-C before use as feeder cells and this was essential for efficient generation of hematopoietic cells. Treatment with mitomycin C may not only inactivate the mitosis of OP9 but also enhance the capacity of OP9 to support hematopoietic differentiation [26].

In Slukvin's method, cells harvested from the 1st step culture were directly transferred to 2-hydroxyethyl methacrylate-coated culture containers for the 2nd step culture. In our method, cells harvested from the 1st step culture were incubated in tissue-culture-coated dishes for 2-5 hours to remove adherent cells. Removal of cells committed to non-mesodermal lineages by this procedure is essential. In addition, the 2nd step culture was also done with OP9 feeder in our method.

After the 2nd step culture, removal of dead cells and aggregated cells may be necessary in Slukvin's method, as described in their report. Indeed, we observed many dead cells as well as DC-like cells, when we tried Slukvin's method. In our method, most of recovered cells after the 2nd step were viable, and removal of dead cells was not necessary.

The issues of safety and efficacy are critical for the establishment of ES-DC therapy. It is presumed that pre-clinical *in vivo* studies with the non-human primates will be required. Therefore, the ability to generate ES-DC from cynomolgus monkey ES cells is also considered to be important. It is probable that ES-DC can be generated from the ES cells of other non-human primates used in medical research, such as the rhesus monkey (*Macaca Murata*) [27] and the common marmoset (*Callithrix jacchus*) [28]. For clinical application of the ES-DC technology, development of feeder-free differentiation method may be required. Embryoid body-mediated differentiation methods may be one way to resolve this issue. In the mouse system,

induction of mesodermal differentiation of ES cells using type IV collagen-coated culture plates has been reported [29, 30]. Several molecules have been reported to be involved in support of hematopoietic cell growth or differentiation by stromal cells [31-33]. Information on the molecular basis of the interaction between differentiating ES cells and feeder cells is valuable for the development of feeder-free differentiation system.

Considering clinical applications, manipulation of function of ES-DC by genetic modification without use of viral vectors, demonstrated in the present study, has significant advantage. However, random integration of multiple copies of transgenes into various genomic loci of ES cells is accompanied with risks such as activation of cellular oncogenes. Thus, a method to integrate transgenes into intended loci of the genome of human ES cells needs to be established.

Previously, we demonstrated a method for efficient targeted integration of expression vectors into specific genomic sites of mouse ES cells, using exchangeable gene-trap vector with Cre-Lox-mediated recombination system [1]. We are now trying to develop a system for targeted integration of transgenes into human ES cell genome. In this system, at first, gene-targeting vector conveying a drug resistance marker gene flanked by lox sequences is introduced and then ES cell clones carrying the vector properly integrated by homologous recombination are selected. Subsequently, expression vectors with lox sequences are introduced by aid of Cre-Lox recombination system. Integration of a single copy of the transgene into the intended locus can be verified by Southern blot analysis. By this strategy, we can obtain ES cell clones with defined genetic modification, thus avoiding risks accompanying the random integration of exogenous genes.

Allogenicity caused by differences in the genetic background between human ES cell lines and the recipients is considered to be a critical problem in medical application of ES-DC. We previously reported that mouse ES-DC administered into semi-allogeneic recipients, sharing one MHC haplotype with the ES-DC, effectively primed antigen-specific cytotoxic T lymphocytes (CTL), suggesting that ES-DC can survive for a period enough to stimulate antigen-specific CTL restricted by the shared MHC class I [4]. However, in the same semi-allogeneic setting, we also observed that 5 times injection of non-antigen-loaded ES-DC significantly reduced the efficiency of priming of antigen-specific CTL induced by the subsequent injection of antigen-loaded ES-DC (unpublished observation). Thus, repetitive stimulation with ES-DC expressing allogeneic MHC may result in activation and expansion of allogeneic MHC class I-reactive CTL, and in such recipients subsequently transferred ES-DC may be rapidly eliminated. Repeated immunization may be required in clinical applications, for example, to induce anti-tumor immunity. Thus, we should resolve the problem of the histoincompatibility between ES cell lines and recipients.

The methods for targeted gene-modification of human ES cells and for targeted chromosome

elimination of mouse ES cells have been developed [34-36]. To overcome the problem of histoincompatibility, genetic modification to inhibit expression of endogenous HLA class I in ES-DC may be effective. Deletion of more than 1,000 kb of entire HLA class I region of human ES cell genome by gene targeting is infeasible by so far available technology. However, disruption of the genes of molecules necessary for the cell surface expression of HLA class I molecules, such as TAP or β 2-microglobulin (β 2M), is presumably feasible. In our plan, we will introduce expression vector encoding for β 2M-linked form of recipient-matched HLA class I heavy chain into TAP1- or β 2M-deficient human ES cells. We are now testing this strategy by using mouse system.

ACKNOWLEDGMENTS

We thank Risa Goswami for the cDNA microarray experiments, the Chemo-Sero-Therapeutic Research Institute for the cynomolgus monkey peripheral blood samples, and Tanabe Seiyaku Co., Ltd. for CMK6.

REFERENCES

1. Senju S, Hirata S, Matsuyoshi H, et al. Generation and genetic modification of dendritic cells derived from mouse embryonic stem cells. *Blood* 2003;101:3501-3508.
2. Fairchild PJ, Brook FA, Gardner RL, et al. Directed differentiation of dendritic cells from mouse embryonic stem cells. *Curr Biol* 2000;10:1515-1518.
3. Matsuyoshi H, Senju S, Hirata S, et al. Enhanced priming of antigen-specific CTLs in vivo by embryonic stem cell-derived dendritic cells expressing chemokine along with antigenic protein: application to antitumor vaccination. *J Immunol* 2004;172:776-786.
4. Fukuma D, Matsuyoshi H, Hirata S, et al. Cancer prevention with semi-allogeneic ES cell-derived dendritic cells. *Biochem Biophys Res Commun* 2005;335:5-13.
5. Matsuyoshi H, Hirata S, Yoshitake Y, et al. Therapeutic effect of alpha-galactosylceramide-loaded dendritic cells genetically engineered to express SLC/CCL21 along with tumor antigen against peritoneally disseminated tumor cells. *Cancer Sci* 2005;96:889-896.
6. Motomura Y, Senju S, Nakatsura T, et al. Embryonic stem cell-derived dendritic cells expressing glypican-3, a recently identified oncofetal antigen, induce protective immunity against highly metastatic mouse melanoma, B16-F10. *Cancer Res* 2006;66:2414-2422.

7. Hirata S, Senju S, Matsuyoshi H, et al. Prevention of Experimental Autoimmune Encephalomyelitis by Transfer of Embryonic Stem Cell-Derived Dendritic Cells Expressing Myelin Oligodendrocyte Glycoprotein Peptide along with TRAIL or Programmed Death-1 Ligand. *J Immunol* 2005;174:1888-1897.
8. Hirata S, Matsuyoshi H, Fukuma D, et al. Involvement of regulatory T cells in the experimental autoimmune encephalomyelitis-preventive effect of dendritic cells expressing myelin oligodendrocyte glycoprotein plus TRAIL. *J Immunol* 2007;178:918-925.
9. Suemori H, Yasuchika K, Hasegawa K, et al. Efficient establishment of human embryonic stem cell lines and long-term maintenance with stable karyotype by enzymatic bulk passage. *Biochem Biophys Res Commun* 2006;345:926-932.
10. Fujioka T, Yasuchika K, Nakamura Y, et al. A simple and efficient cryopreservation method for primate embryonic stem cells. *Int J Dev Biol* 2004;48:1149-1154.
11. Suemori H, Tada T, Torii R, et al. Establishment of embryonic stem cell lines from cynomolgus monkey blastocysts produced by IVF or ICSI. *Dev Dyn* 2001;222:273-279.
12. Suemori H, Nakatsuji N. Growth and differentiation of cynomolgus monkey ES cells. *Methods Enzymol* 2003;365:419-429.
13. Frangioni JV, Neel BG. Solubilization and purification of enzymatically active glutathione S-transferase (pGEX) fusion proteins. *Anal Biochem* 1993;210:179-187.
14. Uemura Y, Senju S, Maenaka K, et al. Systematic analysis of the combinatorial nature of epitopes recognized by TCR leads to identification of mimicry epitopes for glutamic acid decarboxylase 65-specific TCRs. *J Immunol* 2003;170:947-960.
15. Fujita H, Senju S, Yokomizo H, et al. Evidence that HLA class II-restricted human CD4⁺ T cells specific to p53 self peptides respond to p53 proteins of both wild and mutant forms. *Eur J Immunol* 1998;28:305-316.
16. Tabata H, Kanai T, Yoshizumi H, et al. Characterization of self-glutamic acid decarboxylase 65-reactive CD4⁺ T-cell clones established from Japanese patients with insulin-dependent diabetes mellitus. *Hum Immunol* 1998;59:549-560.
17. Fujii S, Senju S, Chen YZ, et al. The CLIP-substituted invariant chain efficiently targets an antigenic peptide to HLA class II pathway in L cells. *Hum Immunol* 1998;59:607-614.
18. Furuya M, Yasuchika K, Mizutani K, et al. Electroporation of cynomolgus monkey embryonic stem cells. *Genesis* 2003;37:180-187.
19. Hasegawa K, Fujioka T, Nakamura Y, et al. A method for the selection of human embryonic stem cell sublines with high replating efficiency after single-cell dissociation. *Stem Cells* 2006;24:2649-2660.
20. Nakano T, Kodama H, Honjo T. Generation of lymphohematopoietic cells from embryonic stem cells in culture. *Science* 1994;265:1098-1101.
21. Itoh T, Ueda Y, Okugawa K, et al. Streptococcal preparation OK432 promotes functional maturation of human monocyte-derived dendritic cells. *Cancer Immunol Immunother* 2003;52:207-214.
22. Nakahara S, Tsunoda T, Baba T, et al. Dendritic cells stimulated with a bacterial product, OK-432, efficiently induce cytotoxic T lymphocytes specific to tumor rejection peptide. *Cancer Res* 2003;63:4112-4118.
23. Freeman GJ, Long AJ, Iwai Y, et al. Engagement of the PD-1 immunoinhibitory receptor by a novel B7 family member leads to negative regulation of lymphocyte activation. *J Exp Med* 2000;192:1027-1034.
24. Zhan X, Dravid G, Ye Z, et al. Functional antigen-presenting leucocytes derived from human embryonic stem cells in vitro. *Lancet* 2004;364:163-171.
25. Slukvin II, Vodyanik MA, Thomson JA, et al. Directed differentiation of human embryonic stem cells into functional dendritic cells through the myeloid pathway. *J Immunol* 2006;176:2924-2932.
26. Zhang WJ, Park C, Arentson E, et al. Modulation of hematopoietic and endothelial cell differentiation from mouse embryonic stem cells by different culture conditions. *Blood* 2005;105:111-114.
27. Thomson JA, Kalishman J, Golos TG, et al. Isolation of a primate embryonic stem cell line. *Proc Natl Acad Sci U S A* 1995;92:7844-7848.
28. Sasaki E, Hanazawa K, Kurita R, et al. Establishment of novel embryonic stem cell lines derived from the common marmoset (*Callithrix jacchus*). *Stem Cells* 2005;23:1304-1313.
29. Nishikawa SI, Nishikawa S, Hirashima M, et al. Progressive lineage analysis by cell sorting and culture identifies FLK1⁺VE-cadherin⁺ cells at a diverging point of endothelial and hemopoietic lineages. *Development* 1998;125:1747-1757.
30. Ogawa M, Kizumoto M, Nishikawa S, et al. Expression of alpha4-integrin defines the earliest precursor of hematopoietic cell lineage diverged from endothelial cells. *Blood* 1999;93:1168-1177.
31. Ueno H, Sakita-Ishikawa M, Morikawa Y, et al. A stromal cell-derived membrane protein that supports hematopoietic stem cells. *Nat Immunol* 2003;4:457-463.
32. Tian X, Morris JK, Linehan JL, et al. Cytokine requirements differ for stroma and embryoid body-